Liu *et al. BMC Biology* (2025) 23:65
https://doi.org/10.1186/s12915-025-02165-3

BMC Biology

RESEARCH

Open Access

Proteomic analysis reveals the alleviation of follicular development defects in offspring mice under DEHP exposure by melatonin

Jing-Cai Liu[1,2], Yuan-Jing Zou[1], Kun-Huan Zhang[1], Yi-Ming Ji[1], Yue Wang[1] and Shao-Chen Sun[1,3*]

Abstract

Background Environmental endocrine disruptor Di (2-ethylhexyl) phthalate (DEHP) widely affects the health of human and animals including the reproductive system. However, there are few studies on the protective strategies for the maternal DEHP exposure on follicular development of offspring. In the present study, we established a model of lactation female mice exposed to DEHP and reported the effects and potential mechanism of melatonin on the follicular development of offspring.

Results Our data showed that melatonin rescued the decrease of primordial follicles, antral follicles and oocyte number (increased by 74.2%) of offspring caused by maternal DEHP exposure from the primordial follicle formation stage. Proteomic analysis showed that melatonin altered the ovarian steroidogenesis, lipid metabolism, signal transduction, and DNA damage-related proteins. Melatonin reversed the disorder of lipid metabolism caused by DEHP and stabilized ovarian hormone secretase level. Molecular docking results indicated that DEHP/MEHP/melatonin binds to HSD17B2 to form a stable conformation, which may explain the reduction in 17β-estradiol induced by DEHP. Moreover, melatonin restored granulosa cell proliferation, reduced oxidative stress and DNA damage-related apoptosis, enhanced mitochondrial function, and protected ovarian cells. Besides, melatonin enhanced gap junction and promoted intercellular communication, which facilitate the formation of primordial follicles and the growth and development of antral follicles. In addition, melatonin rescued the oocyte defects of offspring caused by maternal DEHP exposure.

Conclusions Taken together, our data showed that melatonin could alleviate the damage of follicular development and abnormal ovarian steroidogenesis of offspring caused by maternal DEHP exposure.

Keywords DEHP, Melatonin, Offspring mice, Follicle, Apoptosis, Ovarian steroidogenesis

*Correspondence:
Shao-Chen Sun
sunsc@njau.edu.cn
[1] College of Animal Science and Technology, Nanjing Agricultural University, Nanjing 210095, China
[2] School of Life Sciences, Inner Mongolia University, Hohhot 010021, China
[3] Key Laboratory of Research on Clinical Molecular Diagnosis for High Incidence Diseases in Western Guangxi of Guangxi Higher Education Institutions, Reproductive Medicine of Guangxi Medical and Health Key Discipline Construction Project, Affiliated Hospital of Youjiang Medical University for Nationalities, Baise, China

Background

Di (2-ethylhexyl) phthalate (DEHP) is one of the environmental endocrine disruptors, which is used as a plastic additive in products including clothes, food packaging, intestinal coating of solid oral drugs, coatings, vinyl floor, wall coverings, kitchen accessories, rain gear, toys, medical equipment, and blood storage bags [1, 2]. DEHP from external environment can enter the organism through the respiratory system, digestive system and skin, while the digestive tract absorption through food intake is the largest intake pathway of DEHP [3]. The human DEHP

exposure dose is estimated to be 3–30 μg/kg/day [4, 5]. DEHP and its metabolite MEHP have been detected in humans in different matrices such as saliva, breast milk, blood, urine, and semen and they can also cross the placental barrier [6–8]. DEHP exposure can damage the normal function of nerves, liver, heart, kidney, testis, and ovary [9, 10]. Oxidative stress and DNA damage induced by DEHP exposure were widely observed in hepatocytes, and DEHP exposure in rats also can cause abnormal lipid metabolism and lead to obesity [9, 11, 12].

Besides, DEHP exposure can cause reproductive defects and decreased fertility in mammals. Preterm birth, various pregnancy complications, and endometriosis are all associated with DEHP exposure. In the process of oogenesis and follicular development, DEHP destroys the signal transduction between germ cells and pregranulosa cells by causing oocyte DNA damage and affects the DNA repair ability of homologous chromosome federation in the early stage of meiosis [13, 14]. During primordial follicular formation, DEHP causes elevated levels of oxidative stress and apoptosis and inhibits cyst breakdown and primordial follicle assembly [15]. The upregulation of PDE3A in the ovary of newborn mice induced by DEHP, and the corresponding decrease in the expression levels of cAMP and PKA in oocytes was also the reasons for the decrease of primordial follicle assembly [16]. There was evidence that DEHP induced oxidative stress and DNA damage in various cells, DEHP exposure caused increased DNA damage in mouse sperm and promoted the production of ROS to induce DNA damage in mouse ovarian granulosa cells [17, 18]. DEHP affects the first wave of follicular development in mouse ovaries, and significantly changes the transcription levels of several genes related to immune response and steroidogenesis. Transmission electron microscopy shows the changes in the membrane structure of the membrane cell nucleus, and the number of mitochondria and mitochondrial cristae decrease [19]. Gap junctions are essential for primordial follicle formation and subsequent follicular growth, damage to gap junctions can lead to inhibition of primordial follicle formation, delayed development of antral follicles, and reduced oocyte quality [20, 21]. In the in vitro experiment of female genital ridge, it was found that DEHP exposure could destroy the gap junction and hinder the process of first meiotic division [14]. DEHP exposure also causes a decrease in 17β-estradiol levels in rats, prolongs the duration of the estrous cycle, reduces the number of primary and secondary follicles, and increases follicular atresia [22]. Similarly, the negative effects of DEHP on oocytes are also due to increased DNA damage and apoptosis in the ovary.

The process of ovarian hormone secretion involves the participation of two types of cells and many enzymes. Specifically, after cholesterol enters the theca cells and is internalized into the mitochondrial inner membrane through steroidogenic acute regulatory protein (STAR) [23]. Then, it is converted to pregnenolone by cytochrome P450 side-chain cleavage (CYP11A1) [24]. The synthesized pregnenolone diffuses out of the mitochondria and is transported to the smooth endoplasmic reticulum, where it is converted to progesterone or dehydroepiandrosterone (DHEA) by 3β-hydroxysteroid dehydrogenase (HSD3B) or 17α-hydroxylase/17,20-lyase (CYP17A1), and then these enzymes convert it into androstenedione. Androstenedione can be converted to testosterone by 17β-hydroxysteroid dehydrogenase (HSD17B) or directly spread to granulosa cells and converted to estrone by aromatase (CYP19A1) [25]. The synthesized testosterone and estrone are converted to 17β-estradiol in granulosa cells by CYP19A1 or HSD17B, respectively [5, 26].

Melatonin (N-acetyl-5-methoxytryptamine, MLT) is an endogenous hormone produced by the pineal gland and non-neural tissues and is a key regulator of multiple physiological functions including circadian rhythms and seasonal reproductive activities [27]. Melatonin is also a strong antioxidant, which plays an antioxidant role by removing ROS by itself and its metabolites [28]. Moreover, melatonin promotes DNA repair after being destroyed by free radicals [29]. More and more evidence reveal the protective role of melatonin in the female reproductive system. Melatonin can regulate ovarian function, follicular development, and ovulation by sending photoperiod-dependent signals [30]. And it has a key role in reducing follicular oxidative stress, protecting granulosa cells and oocytes, and thus has a positive contribution to female fertility [31]. Besides, melatonin enhances fertilization-related events by increasing intracellular adenosine triphosphate (ATP) and glutathione (GSH) levels, enhancing the expression of antioxidant genes, regulating the correct cytoplasmic distribution of organelles, and improving bovine oocyte maturation [32]. In mouse ovaries cultured in vitro, the addition of melatonin can alleviate the damage caused by oxidative stress in oocytes and granulosa cells caused by DEHP exposure [15].

Although the effects of DEHP exposure on oogenesis were reported, the protective strategies for the toxicity of DEHP exposure during lactation on the follicular development of offspring are still unclear. In the present study, we established a model of lactation female mice exposed to DEHP and combined it with proteomics to explore the effect of DEHP on the follicular development of offspring and added melatonin to examine its protective effects. Our study contributed to the mechanism of DEHP affecting the follicular development of offspring and the effects

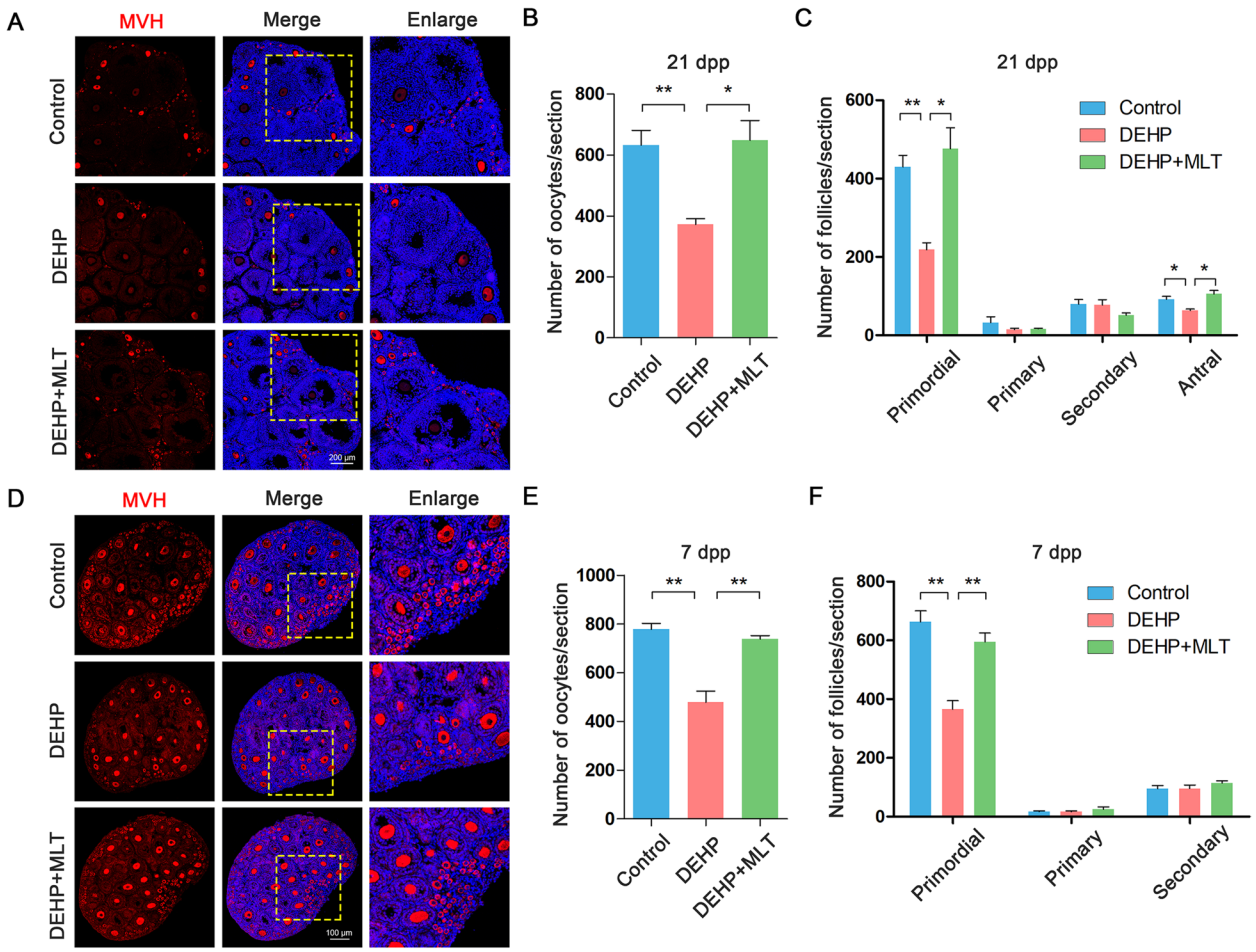

Fig. 1 Melatonin can rescue the total number of oocytes and rescue the loss of primordial follicles and antary follicles caused by DEHP exposure. **A** Representative images of 21 dpp mice ovarian sections labeled with oocyte-specific protein MVH in control group, DEHP group, and DEHP + MLT group. **B** Number of oocytes/section in the ovaries of 21 dpp mice in control group ($n = 3$), DEHP group ($n = 3$), and DEHP + MLT group ($n = 3$). **C** Number of various types of follicles/section in the ovaries of 21 dpp mice in control group ($n = 3$), DEHP group ($n = 3$), and DEHP + MLT group ($n = 3$). **D** Representative images of 7 dpp mice ovarian sections labeled with oocyte-specific protein MVH in control group, DEHP group, and DEHP + MLT group. **E** Number of oocytes/section in the ovaries of 7 dpp mice in control group ($n = 3$), DEHP group, and DEHP + MLT group ($n = 3$). **F** Number of various types of follicles/section in the ovaries of 7 dpp mice in control group ($n = 3$), DEHP group ($n = 3$), and DEHP + MLT group ($n = 3$). Results are expressed as mean ± SEM (**$P < 0.01$;*$P < 0.05$)

of melatonin alleviating the defects caused by DEHP exposure.

Results

Melatonin supplementation alleviates follicular development defects in offspring caused by maternal DEHP exposure

Maternal DEHP exposure affected the formation of primordial follicles and the development of antral follicles in offspring, and the addition of melatonin could alleviate this adverse effect. By analyzing the ovarian sections of 21 dpp offspring female mice, we found that DEHP exposure affected follicular development in offspring mice, and melatonin supplementation alleviated this phenomenon (Fig. 1A). The total number of ovarian oocytes in the melatonin rescue group (DEHP + MLT) was higher than that in the DEHP group (Control = 632.67 ± 48.75; DEHP = 372.33 ± 18.75; DEHP + MLT = 648.67 ± 64.34, Fig. 1B). Through the statistics of various types of follicles, it was found that the number of primary follicles (Control = 429.67 ± 29.34; DEHP = 218 ± 18.48; DEHP + MLT = 476 ± 53.72, Fig. 1C) and antral follicles (Control = 91.67 ± 13.32; DEHP = 63 ± 6.08; DEHP + MLT = 105.33 ± 9.02, Fig. 1C) were restored in the melatonin rescue group. To explore the time point when the total number of follicles decreased, we collected the ovaries of the 3 dpp offspring mice for ovarian sectioning (Additional file 1: Figure S1A). The results

showed that the total number of oocytes in the ovaries of the 3 dpp offspring mice did not change (Additional file 1: Figure S1B). However, the percentage of oocytes in the primordial follicle was significantly reduced and the percentage of oocytes in the cyst was increased in the DEHP group, and the melatonin rescue group was recovered (Additional file 1: Figure S1C). Further analysis of ovarian sections of 7 dpp mice showed that the total number of oocytes in the DEHP group was significantly reduced (Control = 778 ± 24.64; DEHP = 479.33 ± 45; DEHP + MLT = 738 ± 14.57, Fig. 1D and E), and the number of primordial follicles was also significantly reduced (Control = 663 ± 37.04; DEHP = 365.33 ± 29.81; DEHP + MLT = 594.67 ± 30.37, Fig. 1F), which could be rescued by adding melatonin. We also detected the changes of DEHP metabolite MEHP and found that the concentration of MEHP in DEHP group and DEHP + MLT group was significantly increased (Additional file 2: Figure. S2), indicating that the addition of melatonin did not affect the metabolism of MEHP; besides, the concentration in the ovary is higher than that in the serum, indicating that the ovary might enrich MEHP. The results showed that the addition of melatonin could alleviate the inhibition of ovarian cyst breakdown and primordial follicle formation in offspring mice caused by maternal DEHP exposure.

Proteomic analysis reveals that melatonin stabilizes lipid metabolism in offspring under maternal DEHP exposure

To explore the mechanism of melatonin alleviating follicular development damage caused by maternal DEHP exposure, proteomics analysis was carried out. Through the analysis of differential proteins between DEHP group and melatonin rescue group, 207 differential proteins were screened (Additional file 3: Table S1) (The mass spectrometry proteomics data have been deposited to the ProteomeXchange Consortium via the PRIDE partner repository with the dataset identifier PXD060266). The heat map of differential proteins was shown in Fig. 2A. KEGG cluster analysis showed that the processes involved in the differential proteins between the DEHP group and the melatonin rescue group mainly included endocrine system, signal molecules and interaction, lipid metabolism, signal transduction, transport and catabolism, and cell growth and death (Fig. 2B). GO functional enrichment analysis showed the pathways related to steroid metabolism process, response to oxygen-containing compound, hormone biosynthesis and metabolism, and response to lipid (Fig. 2C). KEGG functional enrichment analysis found that the focus was PPAR signaling pathway, metabolism of xenobiotics by cytochrome P450, ovarian steroidogenesis, steroid hormone biosynthesis, chemical carcinogenesis-DNA adducts, fatty acid degradation, and biosynthesis of unsaturated fatty acids and other pathways (Fig. 2D). The enrichment string analysis of the first 15 pathways obtained by KEGG functional enrichment analysis showed that the differential proteins were mainly concentrated in ovarian steroidogenesis and steroid production, cholesterol and lipid metabolism, and cytochrome P450 metabolism and DNA damage (Fig. 2E).

Since several pathways were identified to be related to lipid metabolism in proteomic results, such as cholesterol metabolism, fatty acid metabolism, unsaturated fatty acid biosynthesis, and PPAR signaling pathway, we performed HE staining of the liver of the female offspring and the results showed that the liver cell voids in the DEHP group were larger (Control = 9.35 ± 1.04; DEHP = 15.66 ± 1.20; DEHP + MLT = 9.75 ± 0.34, Fig. 3A, B), indicating the fat accumulation. Through liver Oil Red O staining, it was found that the liver of female offspring in the DEHP group showed a darker lipid droplet color, while the color of the melatonin rescue group was much lighter (Fig. 3C). The relative protein expression level of PPARγ, a protein related to lipid metabolism, was significantly increased in the DEHP group, and significantly decreased in the melatonin rescue group compared with the DEHP group (Control = 1; DEHP = 1.47 ± 0.11; DEHP + MLT = 0.87 ± 0.09, Fig. 3D). The fluorescence intensity of PPARγ in fluorescence immunohistochemistry also showed a similar trend (Control = 20.64 ± 4.17; DEHP = 41.14 ± 2.50; DEHP + MLT = 21.31 ± 2.31, Fig. 3E, F), which further confirmed the lipid accumulation.

Melatonin restores ovarian steroidogenesis and granulosa cell proliferation in offspring under maternal DEHP exposure

Further analysis showed that the gene *Scarb1* related to high-density lipoprotein transport, and the cholesterol-related genes *Star* and *Cyp17a1* were significantly

(See figure on next page.)

Fig. 2 Effects of DEHP exposure and melatonin rescue on ovarian proteomics. **A** Heatmap of differentially expressed proteins in DEHP group and DEHP + MLT group ovaries. **B** KEGG enrichment analysis of differentially expressed proteins in DEHP group and DEHP + MLT group. **C** The top 20 GO enrichment pathways of differentially expressed proteins in DEHP group and DEHP + MLT group. **D** The top 20 KEGG enrichment pathways of differentially expressed proteins in DEHP group and DEHP + MLT group. **E** KEGG Chord Diagram Chord plot shows the genes related to the top 15 KEGG pathways in DEHP group and DEHP + MLT group

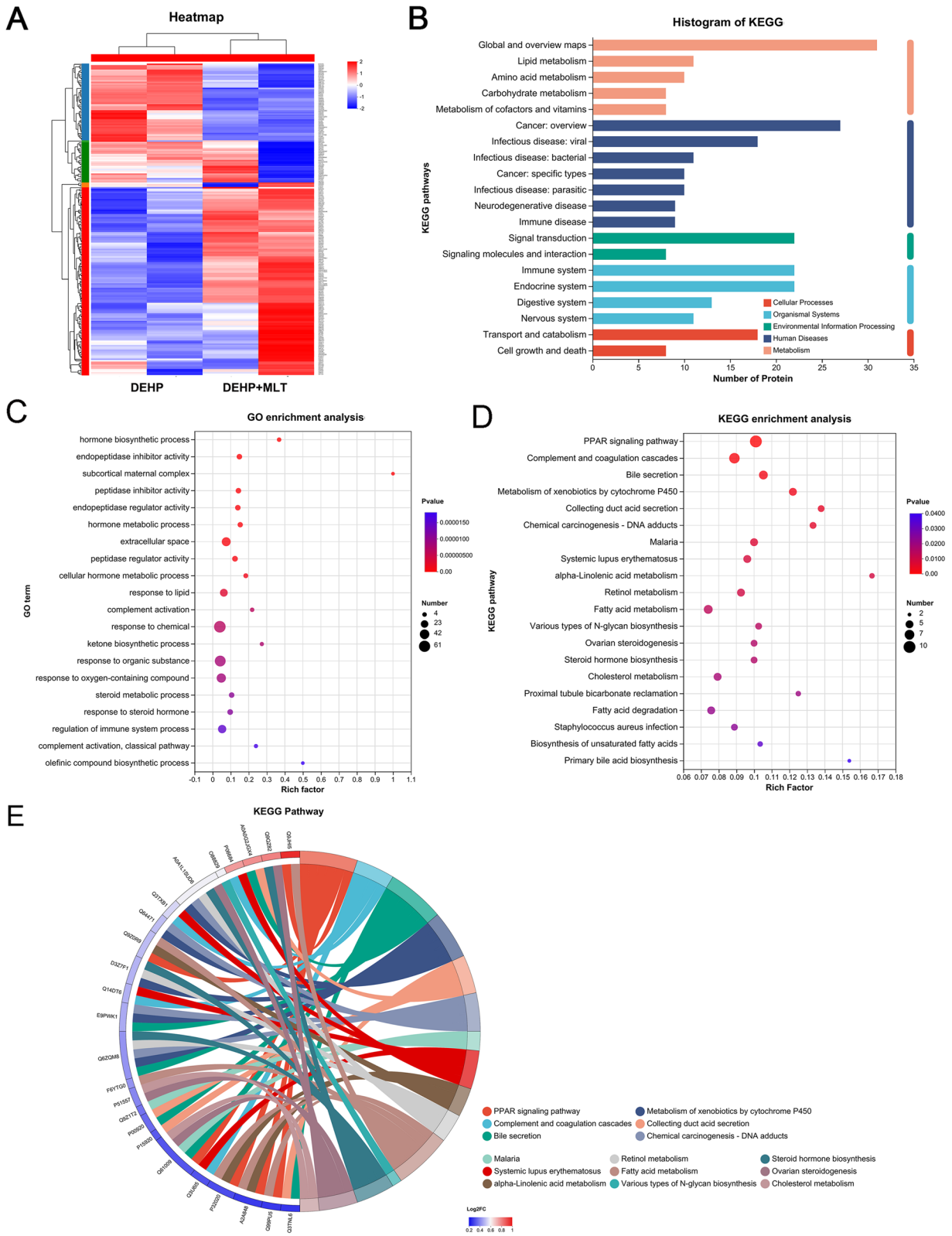

Fig. 2 (See legend on previous page.)

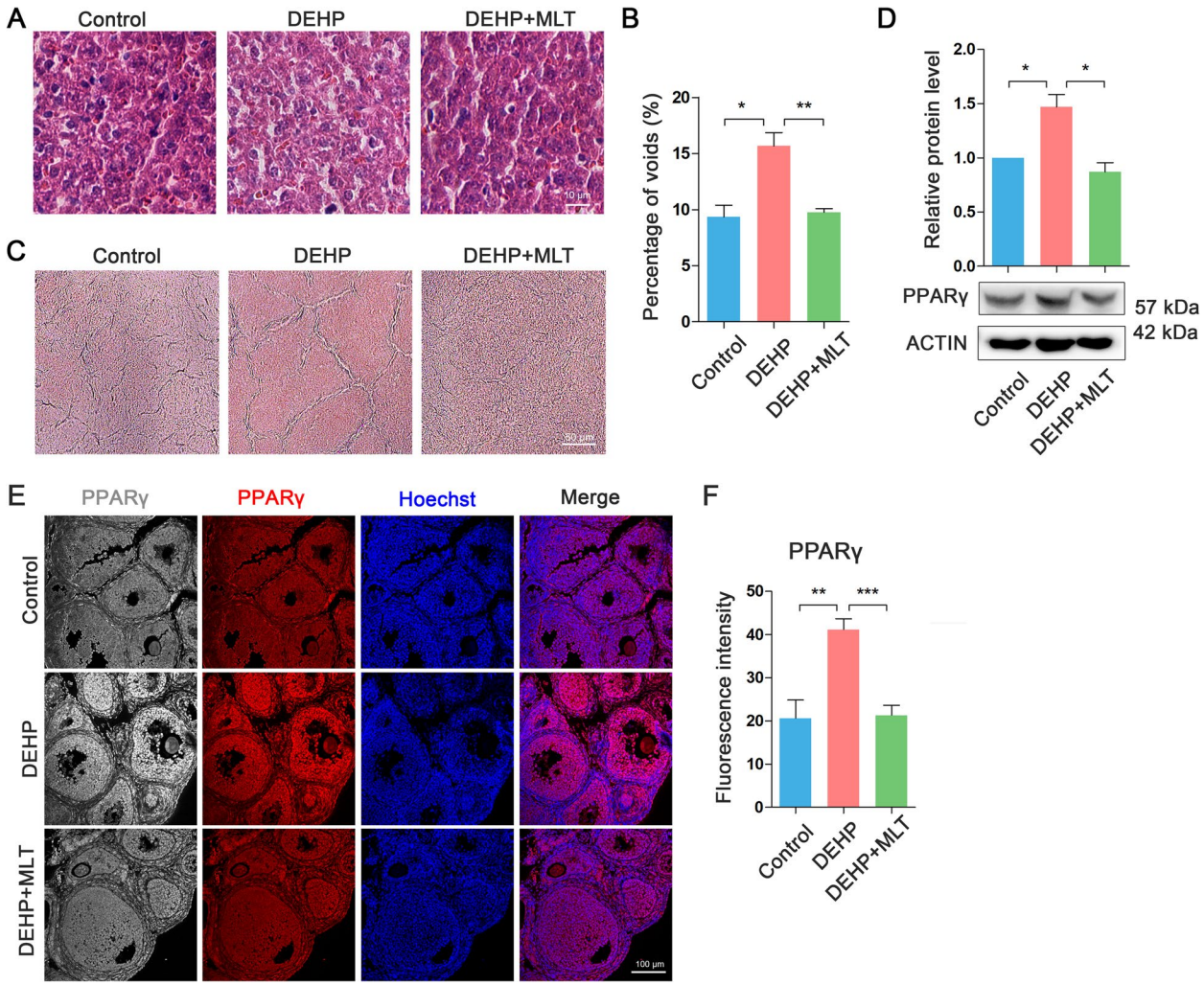

Fig. 3 Melatonin can rescue the effects of lipid metabolism disruption caused by DEHP exposure. **A** HE staining images and **B** the percentage of voids in the liver of mice in control group ($n=3$), DEHP group ($n=3$), and DEHP + MLT group ($n=3$). **C** Oil Red O staining of mice liver in control group ($n=3$), DEHP group ($n=3$), and DEHP + MLT group ($n=3$). **D** The expression level of PPARγ protein in ovary of mice in control group ($n=4$), DEHP group ($n=4$), and DEHP + MLT group ($n=4$). **E, F** The fluorescence intensity of PPARγ protein in ovary of mice in control group ($n=4$), DEHP group ($n=5$), and DEHP + MLT group ($n=8$). Results are expressed as mean ± SEM (***$P<0.001$; **$P<0.01$; *$P<0.05$)

upregulated in the DEHP group, and significantly downregulated after the addition of melatonin, which were also related to ovarian steroidogenesis (Fig. 4A). ELISA detection of E2 in mouse serum showed that melatonin rescue group could significantly increase the level of E2 compared with DEHP group, while DEHP exposure caused a decrease in the level of 17β-estradiol (E2) in offspring (Fig. 4B). We further detected the ovarian steroidogenesis-related proteins and found that the relative protein levels of HSD17B2 and HSD17B10, which were directly related to E2 secretion were significantly reduced after the addition of DEHP, while the addition of melatonin restored their expression levels (HSD17B2: Control = 1; DEHP = 0.61 ± 0.09; DEHP + MLT = 0.93 ± 0.06, HSD17B10: Control = 1; DEHP = 0.60 ± 0.03; DEHP + MLT = 1.19 ± 0.09, Fig. 4C), and the immunofluorescence staining of HSD17B2 also showed the similar results (Control = 24.50 ± 1.19; DEHP = 15.51 ± 0.74; DEHP + MLT = 20.64 ± 0.85, Fig. 4D, E).

We further found that DEHP and its metabolite MEHP have low binding energy with HSD17B2 by molecular docking experiments, and Fig. 5C shows that more amino acids interact with MEHP, which indicated that they can also form stable conformation and compete with estrogen for the receptor, which led to the functional inhibition of HSD17B2 or HSD17B10 (Fig. 5A–C). Melatonin can competitively bind to the adjacent position of DEHP or MEHP in HSD17B2, which will facilitate the protein to

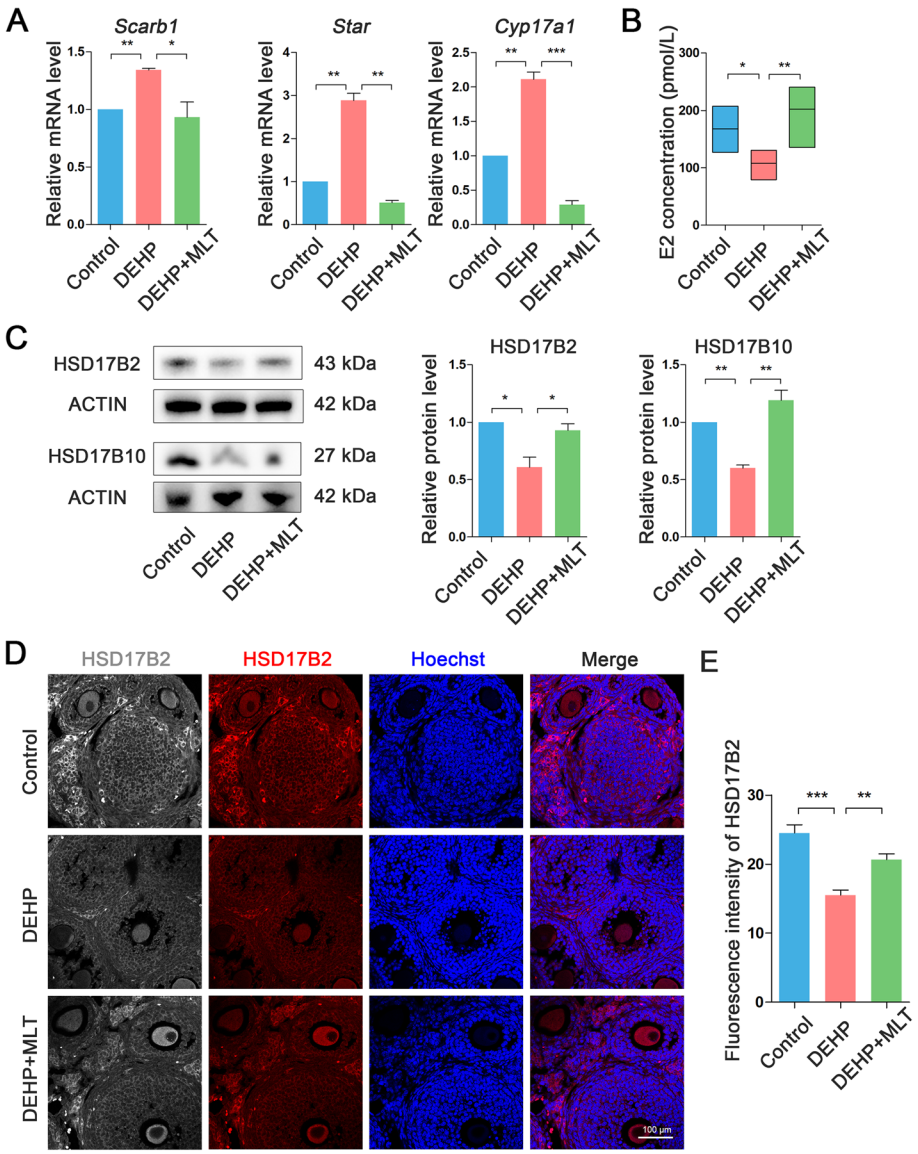

Fig. 4 Melatonin can rescue the effects of ovarian hormone production disruption caused by DEHP exposure. **A** The mRNA levels of genes related to lipid metabolism and ovarian steroidogenesis in ovary of control group ($n=3$), DEHP group ($n=3$), and DEHP + MLT group ($n=3$). **B** E2 concentration in the serum of control group ($n=4$), DEHP group ($n=4$), and DEHP + MLT group ($n=4$). **C** The protein expression levels of HSD17B2 and HSD17B10 in ovary of control group ($n=3$), DEHP group ($n=3$), and DEHP + MLT group ($n=3$). **D** Typical immunofluorescence images and **E** fluorescence intensity analysis of HSD17B2 in ovary of control group ($n=4$), DEHP group ($n=6$), and DEHP + MLT group ($n=5$). Results are expressed as mean ± SEM (***$P<0.001$; **$P<0.01$; *$P<0.05$)

perform its function (Fig. 5D). Since estradiol promotes cell proliferation and DEHP reduces the production of estradiol, immunofluorescence staining was performed for cell proliferation-related protein Ki67 (Fig. 5E). It was found that the Ki67-positive cells in the DEHP group were significantly downregulated. Compared with the DEHP group, the number of Ki67-positive cells in the same area in the melatonin rescue group was significantly upregulated (Control = 83.59 ± 3.00; DEHP = 57.39 ± 1.62; DEHP + MLT = 116.42 ± 4.49, Fig. 5F). These data indicated that melatonin could rescue the inhibition of ovarian granulosa cell proliferation in offspring mice caused by DEHP exposure.

Melatonin enhances mitochondrial function for DNA damage-related ovarian cell apoptosis in offspring under maternal DEHP exposure

From the proteomic analysis, we found that the differentially expressed proteins in the DEHP and melatonin rescue groups were also accumulated in DNA

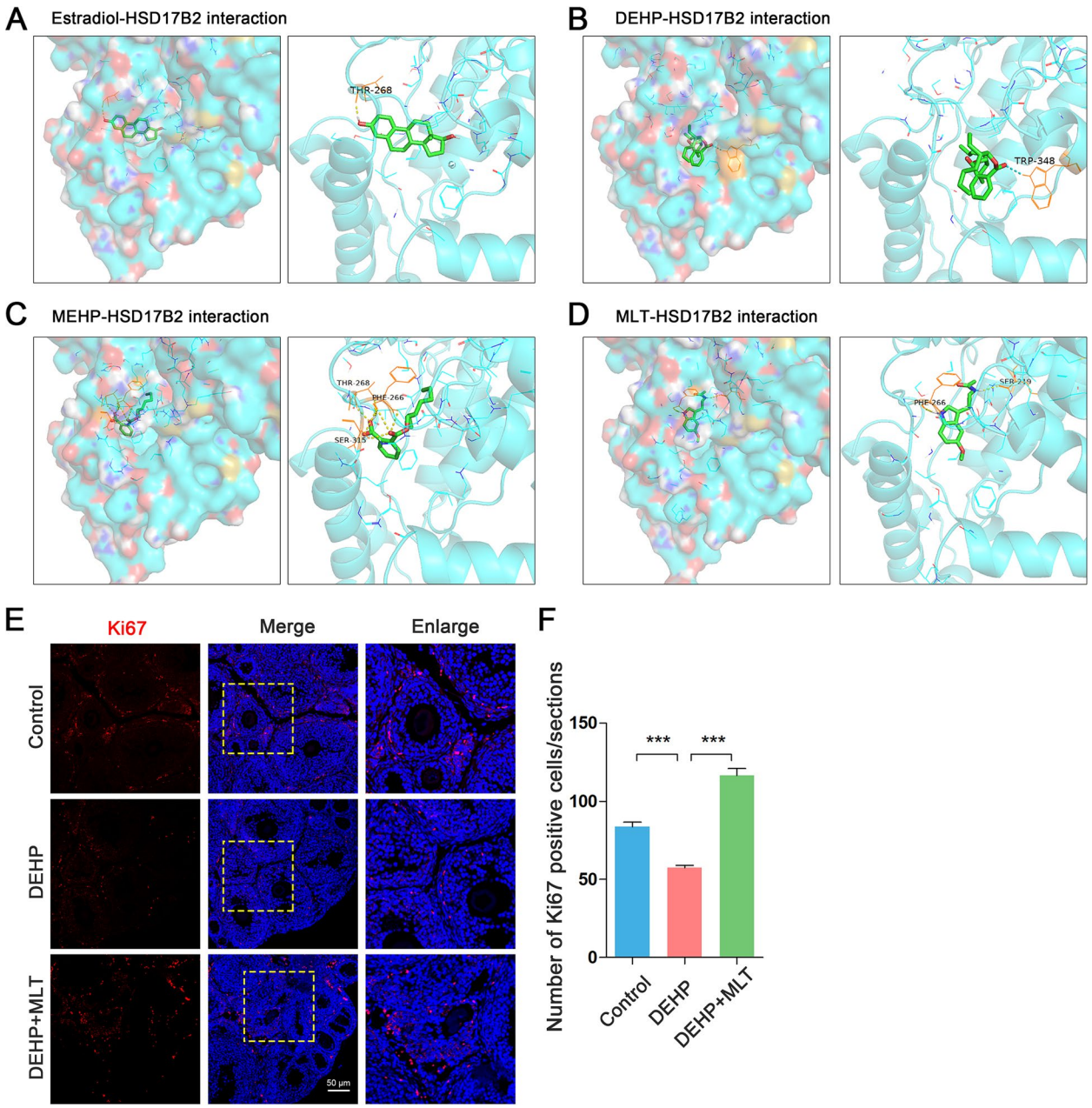

Fig. 5 Molecular docking analysis of Estradiol, DEHP, MEHP, and melatonin with HSD17B2 and rescue analysis of melatonin on DEHP-induced inhibition of ovarian granulosa cell proliferation in mice. **A** Molecular docking analysis of Estradiol with HSD17B2 (−7.7 kcal/mol). **B** Molecular docking analysis of DEHP with HSD17B2 (−6.1 kcal/mol). **C** Molecular docking analysis of MEHP with HSD17B2 (−7.7 kcal/mol). **D** Molecular docking analysis of melatonin with HSD17B2 (−6.2 kcal/mol). **E** Representative images of sections of control group, DEHP group, and DEHP + MLT group ovaries stained for Ki67 (red). **F** The number of Ki67 points in the equal area of ovary in control group ($n = 22$), DEHP group ($n = 18$), and DEHP + MLT group ($n = 12$). Results are expressed as mean ± SEM (***$P < 0.001$)

damage, cytochrome P450 metabolism, and other processes. We showed that compared with the DEHP group, the melatonin rescue group could significantly downregulate the mRNA (Control = 1; DEHP = 2.83 ± 0.37; DEHP + MLT = 0.46 ± 0.10, Fig. 6A) and protein levels (Control = 1; DEHP = 1.89 ± 0.11; DEHP + MLT = 1.02 ± 0.09, Fig. 6B) of the oxidative stress-related protein XDH. We also detected the mitochondrial marker protein TOM20 and found that DEHP significantly downregulated the expression of TOM20 (Control = 1; DEHP = 0.63 ± 0.08; DEHP + MLT = 1.08 ± 0.16, Fig. 6C), which indicates that DEHP exposure caused

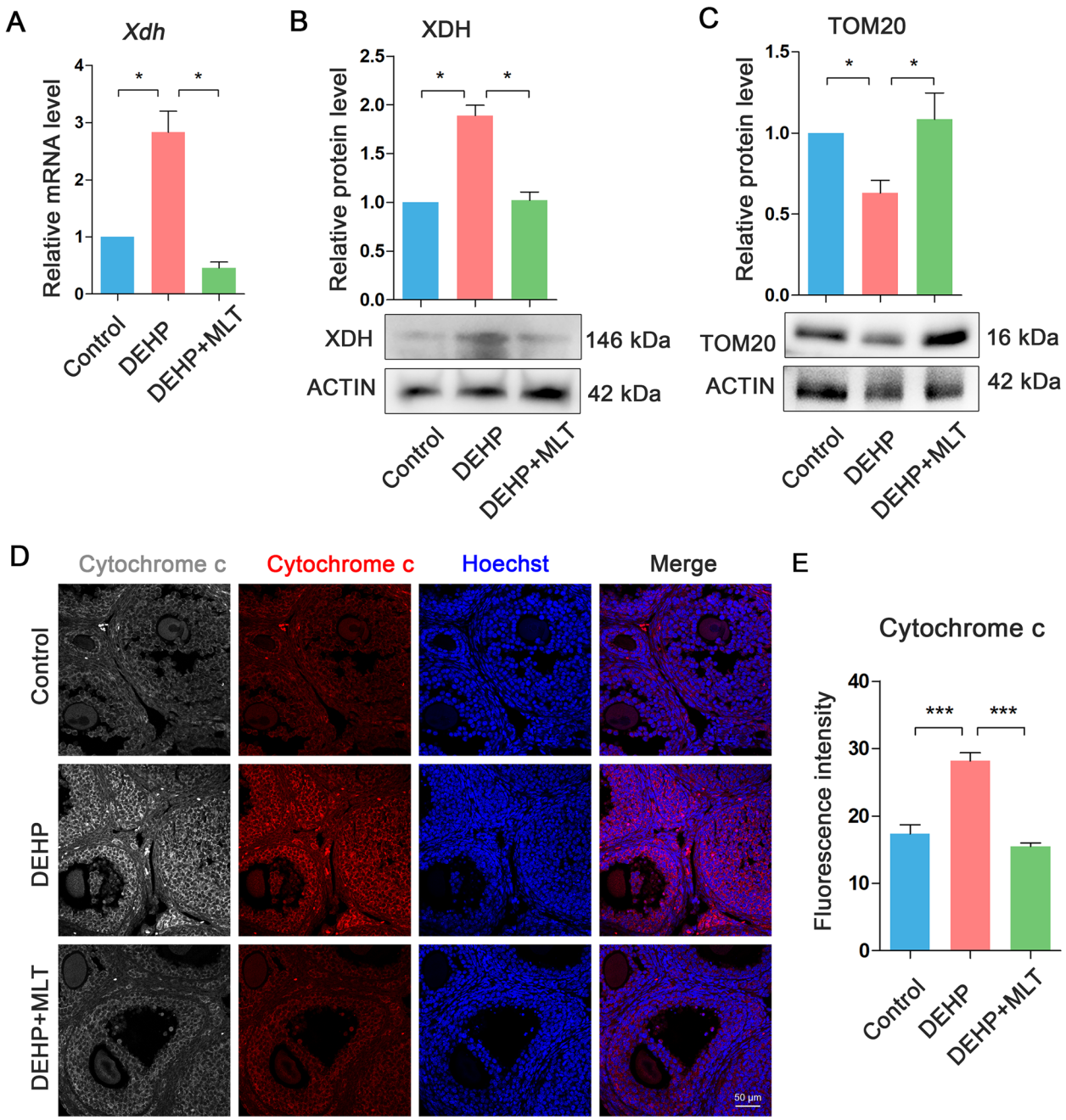

Fig. 6 Melatonin can rescue ROS elevation and mitochondrial damage caused by DEHP exposure. **A** The mRNA level and **B** protein expression level of XDH in ovary of control group ($n=3$), DEHP group ($n=3$), and DEHP + MLT group ($n=3$). **C** Expression levels of mitochondrial related protein TOM20 in ovary of control group ($n=4$), DEHP group ($n=4$), and DEHP + MLT group ($n=4$). **D** Representative images of cytochrome c (red) staining of ovary in control group ($n=5$), DEHP group ($n=6$), and DEHP + MLT group ($n=6$), and **E** fluorescence intensity analysis statistics. Results are expressed as mean ± SEM (***$P<0.001$; *$P<0.05$)

mitochondrial damage, and the addition of melatonin could rescue it. And the immunofluorescence analysis found that the cytochrome c in the DEHP group was significantly upregulated, and the addition of melatonin could restore these defects, suggesting that melatonin improved mitochondrial quality against DEHP exposure through cytochrome c (Control = 17.35 ± 1.32; DEHP = 28.17 ± 1.19; DEHP + MLT = 15.49 ± 0.53, Fig. 6D, E).

The release of cytochrome c and the increase of oxidative stress can lead to DNA damage. Therefore, by

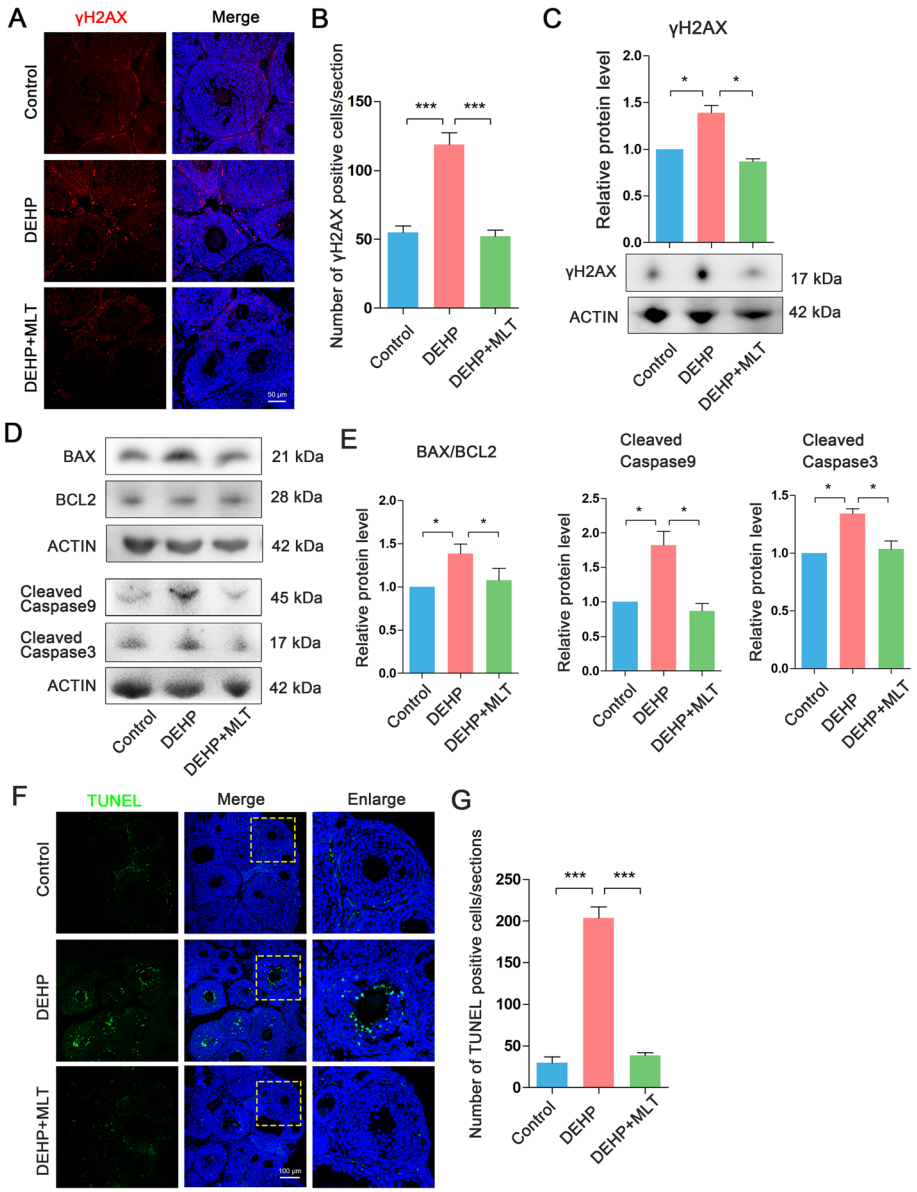

Fig. 7 Melatonin can reduce DNA damage and apoptosis caused by DEHP exposure. **A** Representative images of γH2AX staining (red) and **B** number of γH2AX points in the equal area of the ovary in the control group ($n=6$), DEHP group ($n=6$), and DEHP + MLT group ($n=5$). **C** Representative Western blot and relative protein level of γH2AX. **D** Representative Western blot and **E** relative protein level of BAX/BCL2, Cleaved Caspase9, and Cleaved Caspase3 in ovary of control group ($n=3$), DEHP group ($n=3$), and DEHP + MLT group ($n=3$). **F** Representative TUNEL (red) images and **G** the number of TUNEL-positive cells in the ovaries of 21 dpp female offspring mice in control group ($n=4$), DEHP group ($n=4$), and DEHP + MLT group ($n=8$). Results are expressed as mean ± SEM (***$P<0.001$; *$P<0.05$)

immunofluorescence staining of DNA damage marker γH2AX, we found that the positive signals of γH2AX in the DEHP group were significantly upregulated, while the melatonin rescue group significantly reduced this damage (Control = 55 ± 4.62; DEHP = 118.67 ± 8.83; DEHP + MLT = 52.2 ± 4.57, Fig. 7A, B). Western blot analysis also showed the similar trend (Control = 1; DEHP = 1.39 ± 0.08; DEHP + MLT = 0.87 ± 0.03, Fig. 7C). Next, the level of apoptosis was detected. We found that the protein expression levels of BAX/BCL2, Caspase9, and Caspase3 were significantly upregulated in the DEHP group, and melatonin addition could reduce their expression and inhibit the occurrence of apoptosis (Fig. 7D, E). At the same time, TUNEL assay was detected in the ovaries of 21 dpp mice. In the ovaries of 21 dpp mice, TUNEL-positive cell signals were

significantly upregulated in the DEHP group, and apoptosis was significantly downregulated after melatonin was added (Control = 29.64 ± 7.11; DEHP = 203.58 ± 13.33; DEHP + MLT = 38.57 ± 3.35, Fig. 7F, G). To verify whether early apoptosis also occurred, TUNEL apoptosis was also detected in the ovaries of 3 dpp offspring mice (Additional file 4: Figure S3A) and 7 dpp offspring mice (Additional file 4: Figure S3C). The number of TUNEL positive cells in the DEHP group increased significantly, while the number of TUNEL positive cells decreased significantly after adding melatonin (Additional file 4: Figure S3B and S3D, indicating that DEHP promoted the apoptosis of ovarian cells and affected these stages of follicular development during the cyst breakdown and primordial follicle assembly, and the addition of melatonin reduced the apoptosis of these stages.

Melatonin improves intercellular communication and oocyte quality of offspring under maternal DEHP exposure

Our proteomics results showed that the process of signal transduction was enriched, and the ovarian gap junction protein was involved in information exchange and substance exchange in primordial follicles and antral follicles. Therefore, immunofluorescence staining of gap junction proteins Cx37 and Cx43 was performed. The number of Cx37 (Fig. 8A, B) and Cx43 (Fig. 8C, D) positive cells in the ovaries of offspring mice at 3 dpp and 21 dpp in the DEHP group was significantly reduced. Interestingly, the number of positive cells of Cx37 and Cx43 in the rescue group was significantly higher than that in the DEHP group, which was also increased compared with the control group. This shows that melatonin has a promoting effect on intercellular communication.

Given that DEHP exposure causes increased oxidative stress and apoptosis of the ovary in the offspring, inhibits the development of the primordial follicles and antral follicles, and leads to the breakdown of gap junctions, we further explored whether this adverse effect disrupts the oocyte maturation process and whether the addition of melatonin can rescue this process. We then collected GV oocytes from the 21 dpp offspring mice of control group, DEHP group, and DEHP + MLT group for culture, and found that DEHP exposure caused a decrease in polar body excretion rate, and melatonin could rescue the decrease of polar body extrusion caused by DEHP exposure (Control = 78.97 ± 0.71; DEHP = 69.08 ± 1.84; DEHP + MLT = 76.36 ± 0.80, Fig. 9A). Subsequent detection of MI and MII stage oocytes showed that the DEHP group showed a significant increase in diffuse malformed abnormal spindles and a significant increase in disordered abnormal chromosomes (Fig. 9B). It was found that the addition of melatonin could offset the damage of spindles (Fig. 9C) and chromosomes (Fig. 9D) in MI and MII oocytes caused by DEHP. These findings provide important evidence for oocyte quality protection by melatonin in offspring under DEHP exposure during lactation.

Discussion

In this study, we mainly focused on the rescue effects of melatonin supplementation on the follicular development defects of offspring caused by DEHP exposure during lactation. We found that the addition of melatonin during lactation could downregulate oxidative stress and enhance mitochondrial function to reduce ovarian cell apoptosis; moreover, it could enhance intercellular communication and lipid metabolism and increase estradiol levels to save the offspring follicle development damage, ovarian steroidogenesis, and lipid metabolism disorders caused by maternal DEHP exposure (Fig. 10).

The primordial follicle pool is the embodiment of female reproductive life. The depletion of the follicle pool usually means the beginning of menopause, so the protection of the follicle pool becomes extremely important [33]. The main harmful consequences of DEHP on the ovaries of offspring mice are abnormal follicular development, decreased follicle bank, decreased oocyte quality, and abnormal ovarian steroidogenesis in addition, exposure to DEHP leads to abnormal hormone secretion in mice, rats, pigs, and other animals [19, 34, 35]. Our previous studies have shown that exposure to DEHP during adolescence inhibits the development of antral follicles and leads to the disturbance of hormone secretion [19, 36]. In this study, we found that maternal DEHP exposure significantly reduced the primordial follicle pool of offspring female mice, which seems to be associated with higher DNA damage and apoptosis. Upstream of these effects, DEHP was found to upregulate the oxidative stress-related gene XDH. XDH can be used as a source of ROS, and the upregulation of XDH causes increased oxidative stress and subsequent apoptosis [37]. Studies on the effects of DEHP exposure on the development of primordial follicles and antral follicles also found that XDH was upregulated [15, 38]. This indicates that XDH is a target of DEHP, and the increase of XDH level induces oxidative stress. The consequences of oxidative stress are the release of cytochrome c, mitochondrial damage, DNA damage, and even apoptosis, which have also been confirmed in our study. Many studies have pointed out that oxidative stress in female reproductive organs is the main cause of ovarian aging, which has a negative impact on fertility [39]. As a powerful antioxidant, melatonin assists in the redox balance of mitochondria by reducing superoxide anion molecules on the electron transport chain and the ability to directly scavenge free radicals [40].

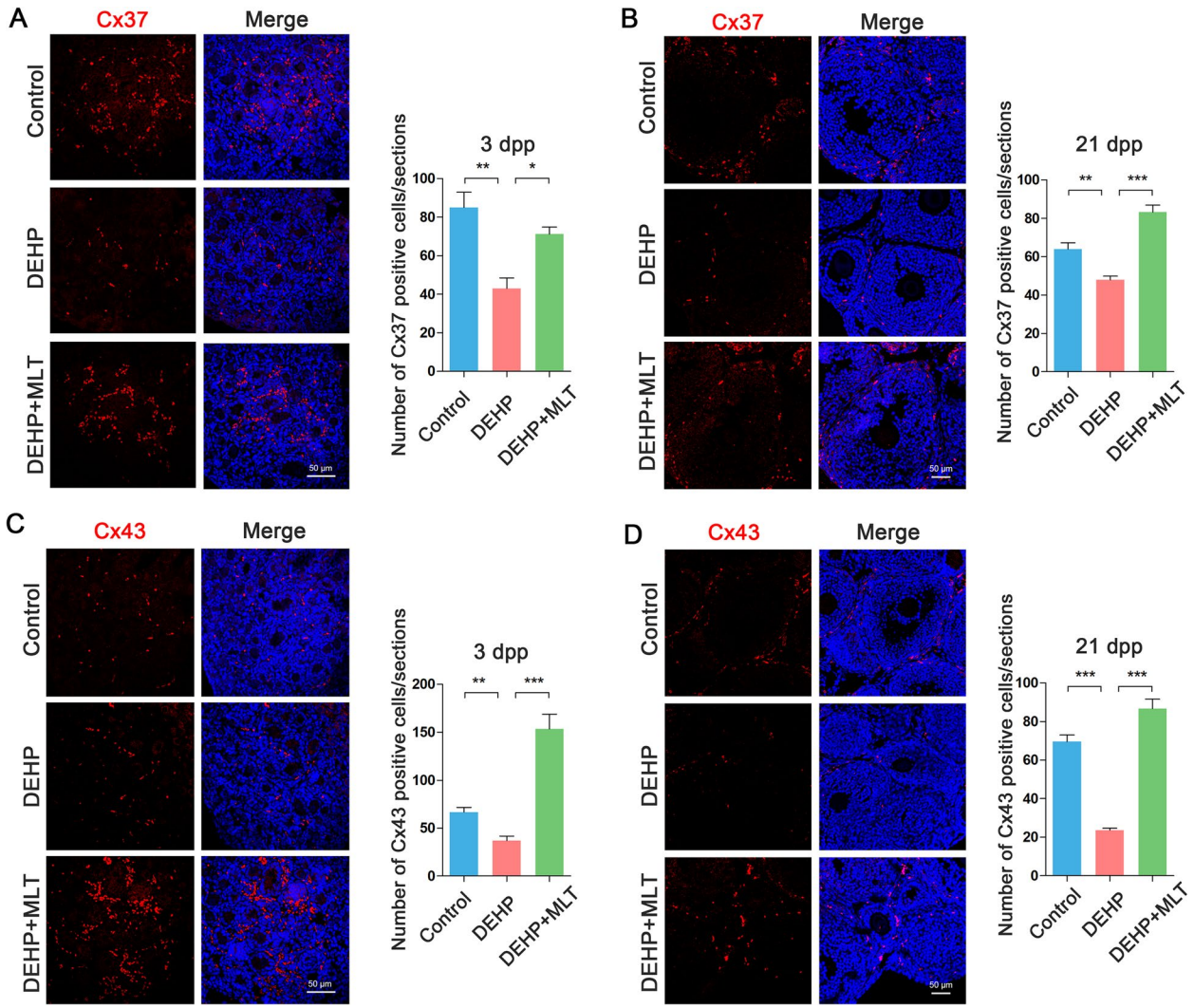

Fig. 8 Adding melatonin enhances cell–cell communication. **A** Representative images of CX37 (red) and the number of positive cells in the ovaries of offspring mice at 3 dpp and **B** 21 dpp days from control group ($n=4$ and 12), DEHP group ($n=5$ and 9), and DEHP + MLT group ($n=3$ and 15). **C** Representative images of CX43 (red) and the number of positive cells in the ovaries of offspring mice at 3 dpp and **D** 21 dpp days from control group ($n=4$ and 8), DEHP group ($n=4$ and 19), and DEHP + MLT group ($n=4$ and 13). Results are expressed as mean ± SEM (***$P<0.001$; **$P<0.01$; *$P<0.05$)

Studies have shown that melatonin treatment reduces the release of mitochondrial cytochrome c and reduces the activation of Caspase-3 and Caspase-9 [41, 42]. In our study, melatonin can rescue the increase of oxidative stress and apoptosis caused by DEHP exposure. Previous studies have shown that the addition of melatonin can reduce the oocyte maturation defects caused by deoxynivalenol, protect early porcine embryos from rotenone-induced mitochondrial defects, and reduce oxidative stress by reducing the expression of XDH to reduce the apoptosis of oocytes and granulosa cells to reduce DEHP-induced follicular development damage [15, 43, 44]. Studies have shown that melatonin can alleviate DEHP-induced inhibition of primordial follicle formation in mice and maintain the survival and activation of sheep primordial follicles through melatonin receptors [15, 45]. This may also be one of the mechanisms we observed that melatonin can alleviate the inhibition of primordial follicle formation induced by DEHP.

In our study, we found that DEHP caused lipid metabolism disorders and decreased 17β-estradiol levels, and genes related to lipid metabolism were also involved in ovarian steroidogenesis. Studies have shown that adolescent exposure to MEHP can lead to elevated cholesterol in mice [46]. We found that the genes that were related to high-density lipoprotein transport, cholesterol, and

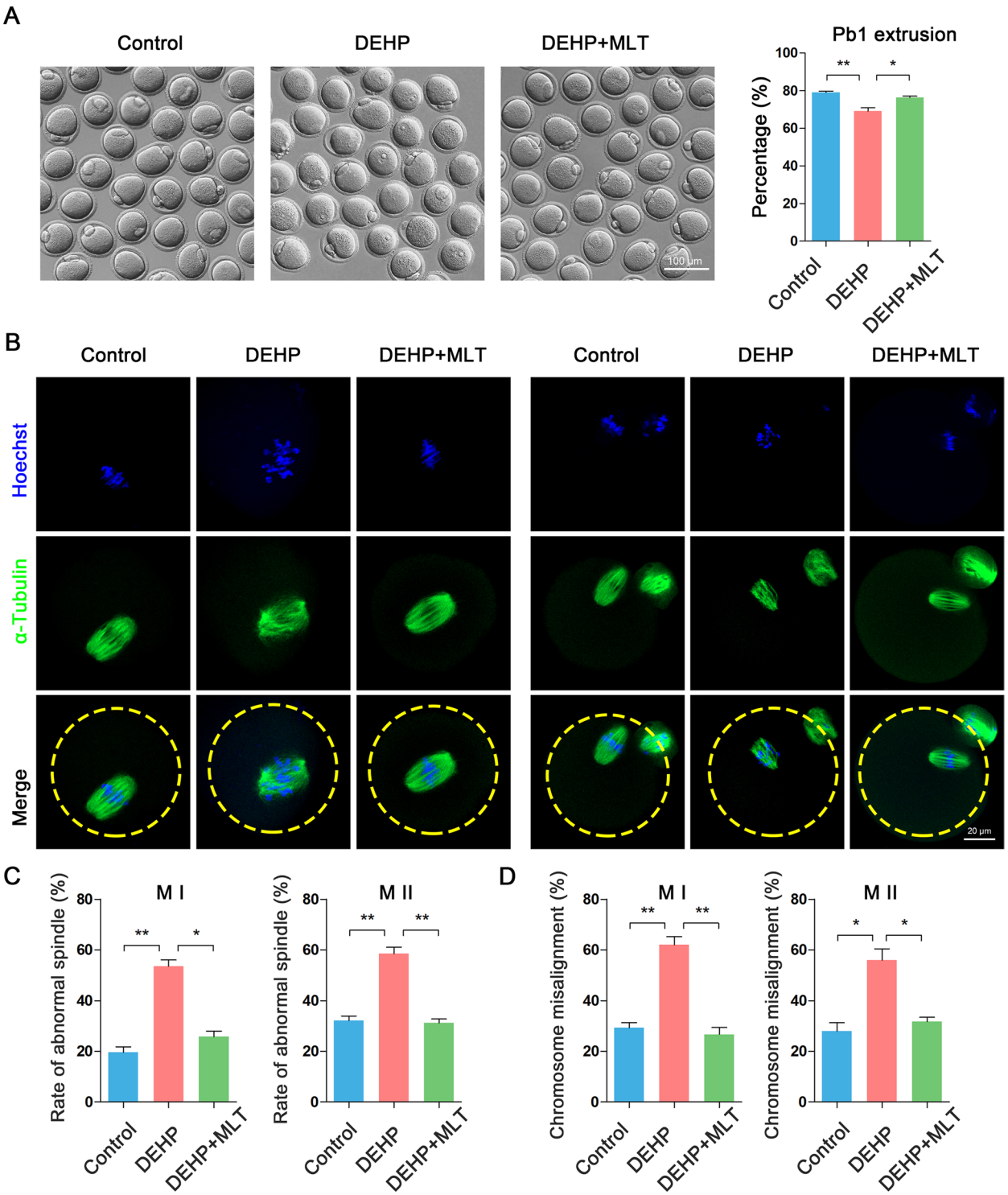

Fig. 9 Melatonin can rescue oocyte spindle abnormalities and chromosome misalignment caused by DEHP exposure. **A** The extrusion rate of the first polar body of oocytes cultured for 12 h in *n* control group ($n = 151$), DEHP group ($n = 165$), and DEHP + MLT group ($n = 106$). **B** Representative images of chromosome and spindle in control group, DEHP group, and DEHP + MLT group. Blue, DNA; Green, α-tubulin. **C** The abnormal rate of spindle in control group ($n = 106$), DEHP group ($n = 97$), and DEHP + MLT group ($n = 95$) in MI or MII. **D** Chromosome misalignment rate in control group ($n = 106$), DEHP group ($n = 97$), and DEHP + MLT group ($n = 95$) in MI or MII. Results are expressed as mean ± SEM (**$P < 0.01$; *$P < 0.05$)

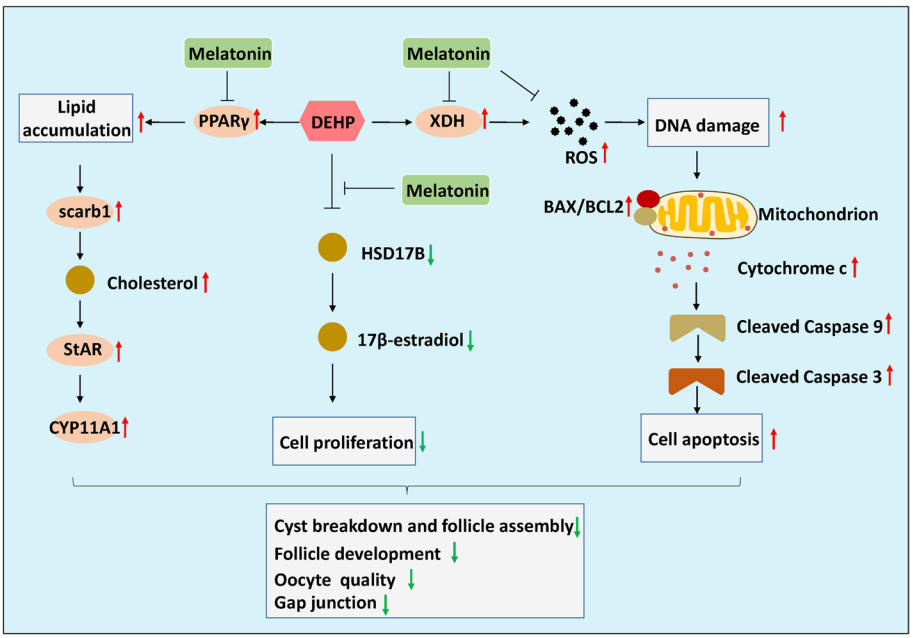

Fig. 10 The regulatory pathways of melatonin alleviate ovarian cell proliferation, apoptosis, lipid accumulation, and decreased 17β-estradiol secretion in offspring mice induced by DEHP exposure during lactation. Melatonin alleviates ROS, DNA damage, and apoptosis induced by DEHP exposure by downregulating the expression of oxidative stress and apoptosis-related protein. Melatonin restores estradiol synthesis by competitively binding DEHP to HSD17B. Melatonin reduces lipid accumulation by downregulating the expression of proteins associated with lipid accumulation. The red arrow represents upregulation, and the blue arrow represents downregulation

ovarian steroidogenesis were significantly upregulated in the DEHP group. It has been reported that PPARγ is involved in follicular growth, ovarian hormones and ovulation secretion, and the increase of PPARγ inhibits the growth of antral follicles [47]. Our results suggest that exposure to DEHP leads to upregulation of *Scarb1* and PPARγ in the ovaries. *Scarb1* is one of the target genes of PPARγ, and the upregulation of PPARγ leads to the upregulation of *Scarb1* [48]. The upregulation of *Scarb1* increases cholesterol into cells, which may be a response to high cholesterol levels in the ovary. Studies have shown that DEHP exposure leads to lipid metabolism disorders and elevated cholesterol in the body [49]. Therefore, we speculate that DEHP leads to the inhibition of lipid metabolism and cholesterol metabolism, which leads to the accumulation of lipid and cholesterol, and then stimulates ovarian cells to transcribe more *Scrb1*, *Star*, and *Cyp17a1* to participate in the ovarian hormone secretion pathway. Melatonin is not only an antioxidant but also a selective estrogen enzyme regulator and plays an important role in reducing cholesterol levels and enhancing lipid metabolism [50–52]. Melatonin-treated oocytes formed smaller lipid droplets and expressed several genes related to lipolysis, which promoted lipid metabolism [53]. We observed that the recovery of liver histology, the decrease of lipid droplets and the decrease of cholesterol-related genes in ovary after melatonin supplementation, indicating that melatonin promoted lipid metabolism and reduced cholesterol levels. One of the functions of HSD17B protein in the estradiol secretion pathway in the ovary is to convert estrone into 17β-estradiol [26]. And the proteome results showed the enrichment of ovarian hormone-related proteins. Although HSD17B2 and HSD17B10 were not screened in the proteome, western results showed that melatonin could alleviate the decrease of HSD17B2 and HSD17B10 caused by DEHP exposure. Through molecular docking experiments, it was found that DEHP and its metabolite MEHP had low binding energy with HSD17B2, which indicated that they could form a stable conformation and compete with estrogen for the receptor, resulting in the functional inhibition of HSD17B2 or HSD17B10. We speculate that DEHP or MEHP acts as an estrogen analog here and binds to HSD17B2 to occupy the position of the original estrogen. This abnormal "estrogen" leads to a decrease in estrogen production and a decrease in estrogen production-related enzyme HSD17B2 through negative feedback. Melatonin can competitively bind to the adjacent position of DEHP or MEHP in HSD17B2, which will facilitate the protein to perform its function. There may also be a case that DEHP caused an increase in ovarian cell apoptosis, and the level of apoptosis decreased after melatonin addition. This may also be due to the increased apoptosis

of granulosa cells caused by DEHP and the decrease of estradiol secretion, while melatonin alleviates the production of apoptosis and restores the secretion of 17β-estradiol. FSH and estradiol affect granulosa cell proliferation by regulating cell cycle [54]. The decrease of 17β-estradiol leads to the decrease of its effect on FSH, which correspondingly reduces the proliferation of granulosa cells and the development of antral follicles. The supplementation of melatonin restores the level of 17β-estradiol, which in turn restores the proliferation of granulosa cells. The results above show that melatonin can not only reduce the oxidative stress and apoptosis level by reducing the expression of oxidative stress-related protein XDH, but also promote lipid metabolism to interfere with the binding of DEHP or MEHP to HSD17B2 and stabilize ovarian steroidogenesis.

In our results, we found that the damage of gap junctions caused by DEHP exposure also led to abnormal follicular development, indicating that DEHP exposure caused inhibition of intercellular information transmission and signal exchange, which might be responsible for the inhibition of cyst breakdown of ovarian germ cells in 3 dpp mice. It seems that DEHP causes gap junction damage in a variety of cells. DEHP exposure causes a decrease in the gap junction protein Cx43, which affects the conduction velocity of cardiomyocytes, and inhibits the gap junction of TM5 supporting cells in mice [55, 56]. DEHP exposure disrupts the gap junction between fetal and postnatal rat testes [57, 58]. Interestingly, the number of Cx37 and Cx43 positive cells in the melatonin rescue group was significantly higher than that in the DEHP group, which was also increased compared with the control group. This shows that melatonin plays an important role in enhancing intercellular communication, which also improves the development ability of subsequent oocytes. DEHP exposure affects ovarian function and oocyte development ability and reduces the proportion of oocytes in horses, cows, mice, and other species entering the MII phase [59–61]. We found that DEHP exposure caused abnormalities in spindles and chromosomes during oocyte maturation, which ultimately affected oocyte maturation. However, in the DEHP group, the decrease in the rate of polar body extrusion did not seem to be more severe than the abnormalities of spindles and chromosomes, which may be related to the lower threshold of microtubule attachment before spindle assembly checkpoint (SAC) inactivation in mammalian oocytes relative to mitotic cells during the metaphase-anaphase transition process [62].

Conclusions

Taken together, we showed that melatonin supplementation not only resisted DEHP-induced oxidative stress and apoptosis, but also regulated ovarian steroidogenesis and stabilized lipid metabolism, which contributed to the protection of the follicular development of offspring during lactation. Since previous studies have shown that the addition of melatonin alone does not affect the formation of primordial follicle, no separate melatonin addition group was involved in this study, which is also a limitation [14]. While the mouse model of this study may not fully reflect the effects of DEHP on human reproductive health. Therefore, subsequent experiments in human cells and clinical statistics are necessary. In addition, it is necessary to investigate whether melatonin is unique or other drugs have similar effects on follicle development damage caused by DEHP.

Methods

Ethics statement

All experiments involving animals were conducted according to the ethical policies and procedures approved by the Animal Management and Ethics Committee of Nanjing Agricultural University, China (Approval no. NJAU.No20220310037).

Animals and experimental design

In this study, we purchased 7-week-old ICR mice from Nanjing Medical University (Nanjing, China). Mice were housed at 22 ± 1°C for 12 h in an alternating light and dark environment and had free access to food and water. The mice were sacrificed by cervical dislocation. Neonatal mice were defined as postnatal day 0 (0 dpp). After birth, the mother mice were given water containing DEHP and melatonin orally until the offspring mice were 21 dpp. The ovaries of 3 dpp, 7 dpp, and 21 dpp offspring mice and the serum of 21 dpp offspring mice were collected for subsequent experiments, a total of 126 mice were used in this study. Based on the human exposure dose and previous studies, we selected DEHP exposure doses of 40 μg/kg/day [4, 5, 36]. The dose of melatonin was set to 2 mg/kg/day according to the published reports and preliminary experimental verification [43, 63]. DEHP stock solution with a concentration of 40 g/L was prepared with dimethyl sulfoxide (DMSO) as a solvent, and then diluted with deionized water to 40 mg/L. Melatonin was dissolved in ethanol and diluted to 2 g/L with deionized water. The female mice were orally administered 1 μL/g/day daily to ensure that the daily DEHP intake dose of the DEHP group was 40 μg/kg/day; in the melatonin rescue group, the DEHP intake was 40 μg/kg/day and the melatonin intake was 2 mg/kg/day. The control group was given deionized water containing the same amount of DMSO and ethanol.

Immunofluorescence histochemistry

Ovarian samples were collected and placed in 4% paraformaldehyde at 4 °C overnight. Subsequently, after

dehydration and paraffin embedding steps, the ovaries were embedded in paraffin blocks, and the ovaries were sliced into standard histological sections of 5 μm thickness. The prepared sections were subjected to xylene dewaxing and gradient alcohol rehydration, followed by antigen repair, and then 100 μL blocking solution was added to each slice and placed at room temperature for 30 min. Fifty microliters of primary antibody diluted with blocking solution overnight at 4 °C was added. Subsequently, 50 μL diluted secondary antibody was added and incubated at 37 °C for 40 min. Hoechst33342 staining solution was added for nuclear labeling. The fluorescence decay-resistant seal tablets (I033-1–1; Nanjing Jiancheng, China) were used to seal the tablets, and a confocal laser scanning microscope (Zeiss, LSM 900 META) was used to image the prepared tablets. For the statistics of the number of follicles, 5-μm slices were made in each ovary. All sections were divided into five parts on average, and one section was taken from each part for counting. We calculated the number of follicles in each of the five sections as the number of follicles in the ovarian section, and each group of data was obtained from the ovary statistics of at least three mice.

Western blot

Ovarian samples were lysed with RIPA lysate to extract proteins. Electrophoresis was performed with 10% NuPAGE Novex prepreg, and then the protein was transferred to PVDF membrane. At 4 °C, the PVDF membrane was blocked in TBST containing 5% skim milk for 4 h, and then incubated with primary antibody (Additional file 5: Table S2) for 12 h at 4 °C. After that, the PVDF membrane was incubated in a diluted secondary antibody for 80 min. Tanon ECL chemiluminescence solution was used for chemiluminescence signal image acquisition, and grayscale quantitative analysis was performed using AlphaView SA software (Proteinsimple, CA, USA). The original uncropped blots are shown in Additional file 6: Fig. S4.

Oocyte culture

For oocyte culture, the ovaries of 21 dpp offspring mice in the control group, DEHP group and DEHP + MLT group were collected. The ovary was manually ruptured with a blade, and then the GV oocytes were collected with an oral pipette. The collected oocytes were washed 6 times with preheated M2 medium. Subsequently, the oocytes were transferred to M2 medium covered with paraffin oil and cultured in a 5% CO_2 incubator at 37 °C. After 12 h of culture, the first polar body extrusion rate was counted.

Immunofluorescence staining of oocytes

The protocol was based on our previous studies [64]. The cultured oocytes were collected and transferred to 100 μL 4% paraformaldehyde at room temperature for 30 min, and then transferred to PBS containing 0.5% Triton X-100 for 20 min. The cells were blocked with PBS containing 1% BSA for 1 h. The oocytes were transferred to the primary antibodies diluted with blocking solution, incubated overnight at 4 °C, washed 3 times with PBS containing 0.1% Tween 20 and 0.01% Triton X-100, and stained with Hoechst33342 for 10 min to label oocyte chromosomes. Finally, the oocytes were transferred to a glass slide for sealing, and observed and photographed using a laser confocal microscope.

TUNEL assay

TUNEL assay was adopted for apoptosis detection using the TUNEL Apoptosis Detection Kit (YEASEN, 40307). The sections were dewaxed with xylene and rehydrated with gradient alcohol, then washed with PBS for 5 min. One hundred microliters Proteinase K working solution was added and incubated at room temperature for 15 min. Then 100 μL TUNEL incubation solution was added and incubated at room temperature for 30 min. After incubation, 50 μL TUNEL labeling solution was added to each slice and incubated at 37 °C for 60 min. The labeled sections were washed 3 times in PBS. Hoechst33342 staining solution was added to mark the nucleus. After sealing with fluorescence decay-resistant seal tablets, image acquisition was performed using a laser confocal microscope. The number of positive apoptotic cells in ovarian section was counted.

Proteomic analysis

Ovarian samples of 21 dpp offspring mice in the DEHP group and DEHP + MLT group were collected and sent to Majorbio (Shanghai, China) for protein extraction, labeled and mixed with TMT (Thermofisher, 90111), and then liquid chromatography tandem mass spectrometry (Easy-nLC 1200 combined with QExactive mass spectrometer) was used. The original file of the mass spectrometer was analyzed by Proteome Discoverer Software 2.2. The screening criteria for significantly differentially expressed proteins are as follows: $P < 0.05$ and FC < 1.2 is an upregulated protein, $P < 0.05$ and FC < 0.83 is a downregulated protein. Differential expression and visualization analysis were performed and completed on the Majorbio platform.

RNA extraction and RT-qPCR

After collecting the ovaries from different groups, total RNA was extracted using the Dynabeads mRNA DIRECT kit (Life Technology, 61011, Beijing, China). Reverse transcription was performed using the PrimeScript 1st Strand cDNA Synthesis Kit (Takara, 6110A,

Dalian, China). The cDNA was diluted to 110 ng/μL with deionized water. The real-time quantitative PCR system was prepared according to the instructions of FastStart Universal SYBR Green Master (ROX) reagent (Roche, 04913850001, Mannheim, Germany). Relative quantitative analysis was performed on a QuantStudio 5 instrument. The relative transcriptional abundance was analyzed by $2^{-\Delta\Delta CT}$ method. Additional file 7: Table S3 shows the primers used in this study.

ELISA

Ten microliters serum of mice in the control group, DEHP group, and DEHP + MLT group was taken and detected by mouse 17β-estradiol (E2) ELISA kit (Feiya-BIO, F5605-A, China) or mouse MEHP ELISA kit (Feiya-BIO, FY30086-B, China). First, the standard was diluted gradient. The blank hole, standard hole, and sample hole were established on the ELISA plate. Fifty microliters of diluted standard substance was added to the standard hole in turn, 40 μL of sample diluent was added to the sample hole first, and then 10 μL of mouse serum was added, mixed, and incubated at 37 °C for 30 min. After washing with washing solution for 5 times, 50 μL enzyme-labeled reagent was added and incubated at 37 °C for 30 min. Wash 5 times after incubation, then add 50 μL of developer A and 50 μL of developer B at 37 °C for 10 min, and finally add 50 μL of termination solution per well. The absorbance of each well was measured at 450 nm, and the concentration of E2 or MEHP was calculated by plotting the standard curve.

Hematoxylin–eosin staining

For HE staining of mouse liver, liver paraffin sections were dewaxed in xylene, rehydrated with gradient alcohol, and then incubated with hematoxylin staining solution for 7 min. Subsequently, the eosin staining solution was stained for 1 min, and then dehydrated with gradient alcohol. Finally, after two xylenes, and then sealed with neutral gum. The image is collected under IX53 microscope (Olympus). The percentage of void area to total area was calculated by Image Pro-Plus 6.0 software.

Oil Red O staining

Oil Red O staining of mouse liver was performed using Modified Oil Red O Staining Kit (C0158S, Beyotime). Firstly, the liver tissue of the left lateral lobe of the mouse was collected and added to the frozen embedding agent, and immediately frozen into the-20 refrigerator to coagulate and form. The liver was cut into tissue sections with a thickness of 10 μm using a freezing microtome and then adhered to a slide. After the section was completed, Oil Red O staining was performed. First, 100 μL of washing solution was added and washed for 30 s. Then 100 μL of Oil Red O staining solution was added for incubation and staining for 20 min. After that time, 100 μL of washing solution was added and washed for 30 s. Sealed with sealing liquid and photographed under the IX53 microscope.

Molecular docking

First, the 2D structures of DEHP and MEHP were downloaded from the PubChem database. Then the protein receptors that need to be docked were downloaded in the AlphaFold Protein Structure Database. Chem3D software was used to convert the 2D structure of DEHP and MEHP into a 3D structure in mol format. PyMOL software was used to remove water and residue ligands from protein receptors. AutoDockTools software was used to hydrogenate the protein receptor. After the processing was completed, the ligand was saved as a file in pdbqt format, and the ligand format was changed to pdbqt format. AutoDockTools software was used to determine the docking position of protein receptors. Molecular docking was performed using the vina program. The ligand and receptor files after docking were analyzed by PyMOL software to view the configuration of the lowest binding energy of the ligand and receptor, analyze the binding site information, and export the image.

Statistical analysis

The data were expressed as mean ± SEM. One-way analysis of variance or T test was used for statistical analysis between each group, and GraphPad Prism5 analysis software was used for statistical analysis. At least 3 biological replicates were performed for each analysis in this study. $P < 0.05$ was considered statistically significant.

Abbreviations

DEHP	Di (2-ethylhexyl) phthalate
STAR	Steroidogenic acute regulatory protein
CYP11A1	Cytochrome P450 side-chain cleavage
HSD3B	3β-Hydroxysteroid dehydrogenase
CYP17A1	17α-Hydroxylase/17,20-lyase
HSD17B	17β-Hydroxysteroid dehydrogenase
ATP	Adenosine triphosphate
GSH	Glutathione
MLT	Melatonin

Supplementary Information

The online version contains supplementary material available at https://doi.org/10.1186/s12915-025-02165-3.

Additional file 1. Figure S1. Melatonin can rescue cyst breakdown inhibition caused by DEHP exposure. (A) Representative images of 3 dpp mice ovarian sections labeled with oocyte specific protein MVH in control group, DEHP group and DEHP+MLT group. (B) Number of oocytes/sections in the ovaries of 3 dpp mice in control group (*n*=3), DEHP group (*n*=3) and DEHP+MLT group (*n*=3). (C) Percentage of cyst and primordial follicles in the ovaries of 3 dpp mice in control group (*n*=3), DEHP group

(*n*=3) and DEHP+MLT group (*n*=3). Results are expressed as mean ± SEM (**$P < 0.01$; *$P < 0.05$).

Additional file 2. Figure S2. DEHP exposure increased MEHP concentrations in serum and ovary of offspring mice. (A) MEHP concentration in serum of offspring mice in control group (*n*=4), DEHP group (*n*=4) and DEHP+MLT group (*n*=4). (B) MEHP concentration in the ovaries of offspring mice in control group (*n*=4), DEHP group (*n*=4) and DEHP+MLT group (*n*=4). Results are expressed as mean ± SEM.

Additional file 3. Table S1. Antibodies used for Western blot and Immunofluorescence analysis.

Additional file 4. Figure S3. Melatonin can reduce ovarian cell apoptosis in 3 dpp and 7 dpp offspring mice. (A) Representative TUNEL (red) images and (B) the number of TUNEL positive cells in the ovaries of 3 dpp female offspring mice in control group (*n*=6), DEHP group (*n*=7) and DEHP+MLT group (*n*=6). (C) Representative TUNEL (red) images and (D) the number of TUNEL positive cells in the ovaries of 7 dpp female offspring mice in control group (*n*=5), DEHP group (*n*=6) and DEHP+MLT group (*n*=4). Results are expressed as mean ± SEM. (***$P < 0.001$).

Additional file 5. Table S2. Primers used for RT-PCR in this study.

Additional file 6. PDF S4. Uncropped original blots used in this study.

Additional file 7. Table S3. Original mass spectrometry data generated for the study.

Additional file 8. Table S4. The supporting data used in this study.

Acknowledgements
This work was supported by the National Key Research and Development Program of China (2023YFD1300502), Natural Science Foundation of Guangxi in China (2025GXNSFAA69655), the Fundamental Research Funds for the Central Universities of China (KYT2024002, KJJQ2025001, RENCAI2024011).

Authors' contributions
JCL, SCS designed the study; JCL conducted the animal experiments and collected the data; YJZ, KHZ, and YMJ contributed to animal experiments; YW analyzed the data; JCL, SCS wrote the manuscript. All authors read and approved the final manuscript.

Funding
This work was supported by the National Key Research and Development Program of China (2023YFD1300502), Natural Science Foundation of Guangxi in China (2025GXNSFAA69655), the Fundamental Research Funds for the Central Universities of China (KYT2024002, KJJQ2025001, RENCAI2024011).

Data availability
All data generated or analysed during this study are included in this published article, its supplementary information files and publicly available repositories. The supporting data used in this study are presented separately in Table S4. The mass spectrometry proteomics data are available via ProteomeXchange with identifier PXD060266.

Declarations

Ethics approval and consent to participate
All experiments involving animals were conducted according to the ethical policies and procedures approved by the Animal Management and Ethics Committee of Nanjing Agricultural University, China (Approval no. NJAU. No20220310037). All authors are consent to participate in this study.

Consent for publication
Not applicable.

Competing interests
The authors declare no competing interests.

Received: 6 August 2024 Accepted: 17 February 2025
Published online: 28 February 2025

References

1. Erythropel HC, Maric M, Nicell JA, Leask RL, Yargeau V. Leaching of the plasticizer di(2-ethylhexyl)phthalate (DEHP) from plastic containers and the question of human exposure. Appl Microbiol Biotechnol. 2014;98(24):9967–81.
2. Martinez-Razo LD, Martinez-Ibarra A, Vazquez-Martinez ER, Cerbon M. The impact of Di-(2-ethylhexyl) Phthalate and Mono(2-ethylhexyl) Phthalate in placental development, function, and pathophysiology. Environ Int. 2021;146:106228.
3. Wang Y, Zhu H, Kannan K. A review of biomonitoring of phthalate exposures. Toxics. 2019;7(2):21.
4. Heudorf U, Mersch-Sundermann V, Angerer J. Phthalates: toxicology and exposure. Int J Hyg Environ Health. 2007;210(5):623–34.
5. Hannon PR, Flaws JA. The effects of phthalates on the ovary. Front Endocrinol. 2015;6:8.
6. Silva MJ, Reidy JA, Herbert AR, Preau JL Jr, Needham LL, Calafat AM. Detection of phthalate metabolites in human amniotic fluid. Bull Environ Contam Toxicol. 2004;72(6):1226–31.
7. Caserta D, Pegoraro S, Mallozzi M, Di Benedetto L, Colicino E, Lionetto L, Simmaco M. Maternal exposure to endocrine disruptors and placental transmission: a pilot study. Gynecological endocrinology : the official journal of the International Society of Gynecological Endocrinology. 2018;34(11):1001–4.
8. Mose T, Mortensen GK, Hedegaard M, Knudsen LE. Phthalate monoesters in perfusate from a dual placenta perfusion system, the placenta tissue and umbilical cord blood. Reprod Toxicol. 2007;23(1):83–91.
9. Jia Y, Liu T, Zhou L, Zhu J, Wu J, Sun D, Xu J, Wang Q, Chen H, Xu F, et al. Effects of Di-(2-ethylhexyl) phthalate on lipid metabolism by the JAK/STAT pathway in rats. Int J Environ Res Public Health. 2016;13(11):1085.
10. Rowdhwal SSS, Chen J. Toxic Effects of Di-2-ethylhexyl Phthalate: An Overview. Biomed Res Int. 2018;2018:1750368.
11. Lin H, Yuan K, Li L, Liu S, Li S, Hu G, Lian QQ, Ge RS. In Utero Exposure to Diethylhexyl Phthalate Affects Rat Brain Development: A Behavioral and Genomic Approach. Int J Environ Res Public Health. 2015;12(11):13696–710.
12. Erkekoglu P, Zeybek ND, Giray BK, Rachidi W, Kizilgun M, Hininger-Favier I, Favier A, Asan E, Hincal F. The effects of di(2-ethylhexyl)phthalate on rat liver in relation to selenium status. Int J Exp Pathol. 2014;95(1):64–77.
13. Tian Y, Zhang Y, Dong PY, Sun YH, Zhao AH, Shen W, Zhang XF. Single-cell transcriptomic profiling to evaluate the effects of Di(2-ethylhexyl)phthalate exposure on early meiosis of female mouse germ cells. Chemosphere. 2022;307(Pt 1): 135698.
14. Liu JC, Lai FN, Li L, Sun XF, Cheng SF, Ge W, Wang YF, Li L, Zhang XF, De Felici M, et al. Di (2-ethylhexyl) phthalate exposure impairs meiotic progression and DNA damage repair in fetal mouse oocytes in vitro. Cell Death Dis. 2017;8(8): e2966.
15. Liu JC, Li L, Yan HC, Zhang T, Zhang P, Sun ZY, De Felici M, Reiter RJ, Shen W. Identification of oxidative stress-related Xdh gene as a di(2-ethylhexyl) phthalate (DEHP) target and the use of melatonin to alleviate the DEHP-induced impairments in newborn mouse ovaries. J Pineal Res. 2019;67(1):e12577.
16. Liu JC, Yan ZH, Li B, Yan HC, De Felici M, Shen W. Di (2-ethylhexyl) phthalate impairs primordial follicle assembly by increasing PDE3A expression in oocytes. Environ Pollut. 2021;270: 116088.
17. Wu H, Liu Q, Yang N, Xu S. Polystyrene-microplastics and DEHP co-exposure induced DNA damage, cell cycle arrest and necroptosis of ovarian granulosa cells in mice by promoting ROS production. The Science of the total environment. 2023;871: 161962.
18. Zhuan Q, Li J, Du X, Zhang L, Meng L, Cheng K, Zhu S, Hou Y, Fu X. Nampt affects mitochondrial function in aged oocytes by mediating the downstream effector FoxO3a. J Cell Physiol. 2022;237(1):647–59.
19. Lai FN, Liu JC, Li L, Ma JY, Liu XL, Liu YP, Zhang XF, Chen H, De Felici M, Dyce PW, et al. Di (2-ethylhexyl) phthalate impairs

steroidogenesis in ovarian follicular cells of prepuberal mice. Arch Toxicol. 2017;91(3):1279–92.
20. Winterhager E, Kidder GM. Gap junction connexins in female reproductive organs: implications for women's reproductive health. Hum Reprod Update. 2015;21(3):340–52.
21. Perez-Armendariz EM, Saez JC, Bravo-Moreno JF, Lopez-Olmos V, Enders GC, Villalpando I. Connexin43 is expressed in mouse fetal ovary. Anat Rec A Discov Mol Cell Evol Biol. 2003;271(2):360–7.
22. Adam N, Brusamonti L, Mhaouty-Kodja S. Exposure of Adult Female Mice to Low Doses of di(2-ethylhexyl) Phthalate Alone or in an Environmental Phthalate Mixture: Evaluation of Reproductive Behavior and Underlying Neural Mechanisms. Environ Health Perspect. 2021;129(1):17008.
23. Christenson LK, Strauss JF 3rd. Steroidogenic acute regulatory protein (StAR) and the intramitochondrial translocation of cholesterol. Biochem Biophys Acta. 2000;1529(1–3):175–87.
24. Stocco DM. StAR protein and the regulation of steroid hormone biosynthesis. Annu Rev Physiol. 2001;63:193–213.
25. Fletcher EJ, Santacruz-Marquez R, Mourikes VE, Neff AM, Laws MJ, Flaws JA. Effects of Phthalate Mixtures on Ovarian Folliculogenesis and Steroidogenesis. Toxics. 2022;10(5):251.
26. Damdimopoulou P, Chiang C, Flaws JA. Retinoic acid signaling in ovarian folliculogenesis and steroidogenesis. Reprod Toxicol. 2019;87:32–41.
27. Hardeland R. Melatonin and the pathologies of weakened or dysregulated circadian oscillators. Journal of pineal research. 2017;62(1):e12377.
28. Tan DX, Manchester LC, Esteban-Zubero E, Zhou Z, Reiter RJ. Melatonin as a Potent and Inducible Endogenous Antioxidant: Synthesis and Metabolism. Molecules. 2015;20(10):18886–906.
29. Majidinia M, Sadeghpour A, Mehrzadi S, Reiter RJ, Khatami N, Yousefi B. Melatonin: a pleiotropic molecule that modulates DNA damage response and repair pathways. J Pineal Res. 2017;63(1):e12416.
30. Reiter RJ, Tan DX, Korkmaz A, Rosales-Corral SA. Melatonin and stable circadian rhythms optimize maternal, placental and fetal physiology. Hum Reprod Update. 2014;20(2):293–307.
31. Tamura H, Jozaki M, Tanabe M, Shirafuta Y, Mihara Y, Shinagawa M, Tamura I, Maekawa R, Sato S, Taketani T, et al. Importance of melatonin in assisted reproductive technology and ovarian aging. Int J Mol Sci. 2020;21(3):1135.
32. Zhao XM, Wang N, Hao HS, Li CY, Zhao YH, Yan CL, Wang HY, Du WH, Wang D, Liu Y, et al. Melatonin improves the fertilization capacity and developmental ability of bovine oocytes by regulating cytoplasmic maturation events. J Pineal Res. 2018;64(1):e12445.
33. Grive KJ, Freiman RN. The developmental origins of the mammalian ovarian reserve. Development. 2015;142(15):2554–63.
34. Mourikes VE, Flaws JA. REPRODUCTIVE TOXICOLOGY: Effects of chemical mixtures on the ovary. Reproduction. 2021;162(5):F91–100.
35. Lee Y, Rattan S, Barakat R, Inman Z, De La Torre KM, Meling DD, Monaco MH, Irudayaraj JM, Cann IK, Ko CJ, et al. Early postnatal exposure to di(2-ethylhexyl) phthalate causes sex-specific disruption of gonadal development in pigs. Reprod Toxicol. 2021;105:53–61.
36. Liu JC, Xing CH, Xu Y, Pan ZN, Zhang HL, Zhang Y, Sun SC. DEHP exposure to lactating mice affects ovarian hormone production and antral follicle development of offspring. J Hazard Mater. 2021;416: 125862.
37. Ashry OM, Hussein EM, Abd El-Azime AS. Restorative role of persimmon leaf (Diospyros kaki) to gamma irradiation-induced oxidative stress and tissue injury in rats. Int J Radiat Biol. 2017;93(3):324–9.
38. Li L, Liu JC, Lai FN, Liu HQ, Zhang XF, Dyce PW, Shen W, Chen H. Di (2-ethylhexyl) Phthalate Exposure Impairs Growth of Antral Follicle in Mice. PLoS ONE. 2016;11(2): e0148350.
39. Carlomagno G, Minini M, Tilotta M, Unfer V. From implantation to birth: insight into molecular melatonin functions. Int J Mol Sci. 2018;19(9):2802.
40. Reiter RJ, Tan DX, Rosales-Corral S, Galano A, Zhou XJ, Xu B. Mitochondria: Central Organelles for Melatonin's Antioxidant and Anti-Aging Actions. Molecules. 2018;23(2):509.
41. Yang M, Li L, Chen S, Li S, Wang B, Zhang C, Chen Y, Yang L, Xin H, Chen C, et al. Melatonin protects against apoptosis of megakaryocytic cells via its receptors and the AKT/mitochondrial/caspase pathway. Aging. 2020;12(13):13633–46.
42. Baydas G, Reiter RJ, Akbulut M, Tuzcu M, Tamer S. Melatonin inhibits neural apoptosis induced by homocysteine in hippocampus of rats via inhibition of cytochrome c translocation and caspase-3 activation and by regulating pro- and anti-apoptotic protein levels. Neuroscience. 2005;135(3):879–86.
43. Lan M, Han J, Pan MH, Wan X, Pan ZN, Sun SC. Melatonin protects against defects induced by deoxynivalenol during mouse oocyte maturation. J Pineal Res. 2018;65(1): e12477.
44. Niu YJ, Zhou W, Nie ZW, Shin KT, Cui XS. Melatonin enhances mitochondrial biogenesis and protects against rotenone-induced mitochondrial deficiency in early porcine embryos. J Pineal Res. 2020;68(2): e12627.
45. Barberino RS, Macedo TJS, Lins T, Menezes VG, Silva RLS, Monte APO, Palheta RC Jr, Smitz JEJ, Matos MHT. Immunolocalization of melatonin receptor type 1 in the sheep ovary and involvement of the PI3K/Akt/FOXO3a signaling pathway in the effects of melatonin on survival and in vitro activation of primordial follicles. Mol Reprod Dev. 2022;89(10):485–97.
46. Wang C, Yue S, Hao Z, Ren G, Lu D, Zhang Q, Zhao M. Pubertal exposure to the endocrine disruptor mono-2-ethylhexyl ester at body burden level caused cholesterol imbalance in mice. Environ Pollut. 2019;244:657–66.
47. Ferst JG, Rovani MT, Dau AMP, Gasperin BG, Antoniazzi AQ, Bordignon V, Oliveira DE, Goncalves PBD, Ferreira R. Activation of PPARG inhibits dominant follicle development in cattle. Theriogenology. 2020;142:276–83.
48. Minge CE, Robker RL, Norman RJ. PPAR Gamma: Coordinating Metabolic and Immune Contributions to Female Fertility. PPAR Res. 2008;2008: 243791.
49. Huang YQ, Tang YX, Qiu BH, Talukder M, Li XN, Li JL. Di-2-ethylhexyl phthalate (DEHP) induced lipid metabolism disorder in liver via activating the LXR/SREBP-1c/PPARalpha/gamma and NF-kappaB signaling pathway. Food and chemical toxicology : an international journal published for the British Industrial Biological Research Association. 2022;165: 113119.
50. Tung YT, Chiang PC, Chen YL, Chien YW. Effects of Melatonin on Lipid Metabolism and Circulating Irisin in Sprague-Dawley Rats with Diet-Induced Obesity. Molecules. 2020;25(15):3329.
51. Alizadeh M, Karandish M, Asghari Jafarabadi M, Heidari L, Nikbakht R, Babaahmadi Rezaei H, Mousavi R. Metabolic and hormonal effects of melatonin and/or magnesium supplementation in women with polycystic ovary syndrome: a randomized, double-blind, placebo-controlled trial. Nutr Metab. 2021;18(1):57.
52. Cos S, Gonzalez A, Martinez-Campa C, Mediavilla MD, Alonso-Gonzalez C, Sanchez-Barcelo EJ. Melatonin as a selective estrogen enzyme modulator. Curr Cancer Drug Targets. 2008;8(8):691–702.
53. Jin JX, Lee S, Taweechaipaisankul A, Kim GA, Lee BC. Melatonin regulates lipid metabolism in porcine oocytes. J Pineal Res. 2017;62(2):e12388.
54. Edson MA, Nagaraja AK, Matzuk MM. The mammalian ovary from genesis to revelation. Endocr Rev. 2009;30(6):624–712.
55. Gillum N, Karabekian Z, Swift LM, Brown RP, Kay MW, Sarvazyan N. Clinically relevant concentrations of di (2-ethylhexyl) phthalate (DEHP) uncouple cardiac syncytium. Toxicol Appl Pharmacol. 2009;236(1):25–38.
56. Kang KS, Lee YS, Kim HS, Kim SH. DI-(2-ethylhexyl) phthalate-induced cell proliferation is involved in the inhibition of gap junctional intercellular communication and blockage of apoptosis in mouse Sertoli cells. J Toxicol Environ Health A. 2002;65(5–6):447–59.
57. Di Lorenzo M, Winge SB, Svingen T, De Falco M, Boberg J. Intrauterine exposure to diethylhexyl phthalate disrupts gap junctions in the fetal rat testis. Current research in toxicology. 2020;1:5–11.
58. Sobarzo CM, Lustig L, Ponzio R, Suescun MO, Denduchis B. Effects of di(2-ethylhexyl) phthalate on gap and tight junction protein expression in the testis of prepubertal rats. Microsc Res Tech. 2009;72(11):868–77.
59. Ambruosi B, Uranio MF, Sardanelli AM, Pocar P, Martino NA, Paternoster MS, Amati F, Dell'Aquila ME. In vitro acute exposure to DEHP affects oocyte meiotic maturation, energy and oxidative stress parameters in a large animal model. PLoS ONE. 2011;6(11):e27452.
60. Kalo D, Hadas R, Furman O, Ben-Ari J, Maor Y, Patterson DG, Tomey C, Roth Z. Carryover Effects of Acute DEHP Exposure on Ovarian Function and Oocyte Developmental Competence in Lactating Cows. PLoS ONE. 2015;10(7): e0130896.
61. Zhang XF, Zhang LJ, Li L, Feng YN, Chen B, Ma JM, Huynh E, Shi QH, De Felici M, Shen W. Diethylhexyl phthalate exposure impairs follicular development and affects oocyte maturation in the mouse. Environ Mol Mutagen. 2013;54(5):354–61.
62. Nagaoka SI, Hodges CA, Albertini DF, Hunt PA. Oocyte-specific differences in cell-cycle control create an innate susceptibility to meiotic errors. Curr Biol : CB. 2011;21(8):651–7.

63. Zhang M, Lu Y, Chen Y, Zhang Y, Xiong B. Insufficiency of melatonin in follicular fluid is a reversible cause for advanced maternal age-related aneuploidy in oocytes. Redox Biol. 2020;28: 101327.
64. Hu L-L, Liao M-H, Liu Y-X, Xing C-H, Nong L-L, Yang F-L, Sun S-C. Loss of AMPK activity induces organelle dysfunction and oxidative stress during oocyte aging. Biol Direct. 2024;19(1):29.

Publisher's Note